phys. stat. sol. (b) **245**, No. 12, 2630–2635 (2008) / **DOI** 10.1002/pssb.200844226

physica status solidi b
www.pss-b.com
basic solid state physics

A comparison of polycrystalline elastic properties computed by analytic homogenization schemes and FEM

W. A. Counts[1], M. Friák[1], C. C. Battaile[2], D. Raabe[*,1], and J. Neugebauer[1]

[1] Max-Planck-Institut für Eisenforschung GmbH, Max-Planck-Straße 1, 40237 Düsseldorf, Germany
[2] Computational Materials Science and Engineering Department, Sandia National Laboratories, P.O. Box 5800, Albuquerque, NM 87185-1411, USA

Received 30 May 2008, revised 5 September 2008, accepted 16 September 2008
Published online 7 November 2008

PACS 02.70.Dh, 31.15.E–, 62.20.de, 81.05.Bx, 87.10.Pq

[*] Corresponding author: e-mail d.raabe@mpie.de, Phone: +49-211-6792 278, Fax: +49-211-6792 333

Body-center-cubic (BCC) magnesium–lithium alloys are a promising light-weight structural material. As a first step in a theoretically guided materials design strategy single crystal elastic coefficients for BCC magnesium-lithium alloys with different compositions were computed using ab initio methods. These single crystal elastic coefficients were then used to predict the corresponding polycrystalline elastic properties using various analytic homogenization techniques (Voigt, Reuss, and a self-consistent approach) as well as the finite element method. As expected, the Voigt and Reuss bounds form the upper and lower bounds on the polycrystalline elastic properties, which the predicted values of the self-consistent approach and finite element approaches fall in between. Additionally, the difference between the polycrystalline elastic properties derived from the self-consistent approach and the finite element method is small illustrating the power and value of the self-consistent approach for non-textured materials.

1 Introduction Magnesium-lithium alloys have the potential to be one of the lightest possible metallic alloy systems. The density of Mg–Li alloys is expected to range between 1.74 g/cm^3 (ρ_{Mg}) and 0.58 g/cm^3 (ρ_{Li}). An additional benefit of alloying Mg with Li is that Li stabilizes the body-centered-cubic (BCC) structure over the hexagonal closed packed (HCP) structure with as little as 30 at% Li. Since BCC materials are generally more ductile at room temperature than HCP materials, they are favored in manufacturing operations that require room or low-temperature forming operations.

While there is little doubt that BCC Mg–Li alloys will be light-weight, it is unclear whether these alloys will offer advantageous polycrystalline elastic properties. As part of a theoretically guided materials design strategy, the single crystal elastic constants of various BCC Mg–Li alloys were calculated using density-functional theory (DFT) [1]. However, there remains the problem of calculating the macro-scale polycrystalline elastic properties (like Young's and shear modulus) from the single crystal elastic coefficients (C_{ij}'s) calculated at the atomistic level. To solve this problem, a multi-scale approach is needed that starts at the atomistic level and spans across the grain size level (typically between 10–100 μm for engineering polycrystals) to the macroscale polycrystal level that includes on the order of 10^8 grains.

It is possible to estimate the polycrystalline elastic properties using various analytic homogenization techniques (like Voigt, Reuss, and the self-consistent approach) as well as the finite element method (FEM). These analytic approaches make assumptions on the stress–strain state or geometry of the polycrystal in order to derive simple closed form solutions. The advantage of FEM is that no such assumptions are necessary. In this paper, the usefulness of the analytic estimates of polycrystalline elastic properties for materials with cubic symmetry is investigated. The polycrystalline Young's modulus, shear modulus, and Poisson's ratio of BCC Mg–Li alloys are

estimated using both analytic homogenization techniques and FEM from the same ab initio predicted single crystal data and then compared.

2 Computational methods

2.1 Ab initio calculation of single crystal elastic constants DFT calculations [2, 3] were performed using a plane wave pseudopotential approach as implemented in the Vienna Ab-initio Simulation Package (VASP) code [4, 5]. The exchange correlation was described by PBE-GGA [6] and the Projector Augmented Wave (PAW) method [7] was used to describe Mg (where the 2p and 3s electrons were considered valence) and Li (where the 2s electron was considered valence). Binary alloys were described by cubic $2 \times 2 \times 2$ supercells containing a total of 16 atoms. The plane wave cutoff energy was set to 260 eV and a $16 \times 16 \times 16$ Monkhorst–Pack mesh was used to sample the Brillouin zone.

The ground state properties ($T = 0$ K) of pure BCC Li and Mg as well as 11 alloy compositions were studied. Alloy compositions ranged from 6.25 at% Li (one Li atom in a 16 atom supercell) to 93.75 at% Li (15 Li atoms in a 16 atom supercell). In each case, only one local atomic arrangement was considered for each composition. These atomic arrangements were chosen in a manner that preserved cubic symmetry. This choice allows the direct determination of all the BCC alloy's elastic properties. Four of these ordered structures are shown in Fig. 1. In the present study, only one ordered structure at each concentration was considered due to computational limitations. While the local atomic arrangement is expected to affect the magnitude of the elastic properties, it is not expected to greatly affect the compositional trends, which are the primary concern of this study.

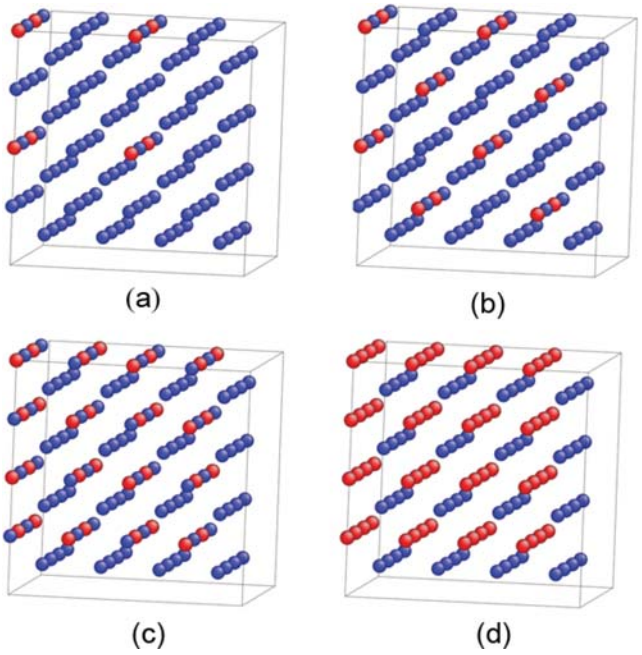

Figure 1 (online colour at: www.pss-b.com) Atomic arrangments of ordered BCC alloys with (a) 6.25 at% solute, (b) 12.5 at% solute, (c) 25 at% solute, (d) 50 at% solute.

The three independent elastic coefficients of a single-crystal with cubic symmetry were determined by distorting the BCC supercell in three different ways [8]. The first distortion is the isotropic volume change from which the single crystal bulk modulus is determined. The single crystal bulk modulus for materials with cubic symmetry can be expressed as a linear combination of C_{11} and C_{12}

$$B_{\text{cubic}} = \frac{C_{11} + 2C_{12}}{3}. \tag{1}$$

The second distortion into a tetragonal structure (ε^{tet}) and the third distortion into a trigonal one (ε^{tri}) are defined as

$$\varepsilon^{\text{tet}} = \begin{pmatrix} -\delta/2 & 0 & 0 \\ 0 & -\delta/2 & 0 \\ 0 & 0 & \delta \end{pmatrix}, \qquad \varepsilon^{\text{tri}} = \begin{pmatrix} 0 & \delta & 0 \\ \delta & 0 & 0 \\ 0 & 0 & 0 \end{pmatrix}, \tag{2}$$

where δ is the distortion. In all ab initio calculations, δ was limited to ±4%. Both ε^{tet} and ε^{tri} lead to changes in the total energy density of the system as a function of δ. The change in the total energy density of the distorted system is defined as the strain energy density

$$U^{\text{tet}} = \frac{E^{\text{tet}} - E_0}{V_0}, \qquad U^{\text{tri}} = \frac{E^{\text{tri}} - E_0}{V_0}, \tag{3}$$

where U^{tet} and U^{tri} are the strain energy densities of the tetragonal and trigonal distorted structures, E^{tet} and E^{tri} are the energies of the tetragonal and trigonal distorted structures, E_0 is the energy of the undistorted structure, and V_0 is the volume of the undistorted structure. The U^{tet} and U^{tri} data was plotted as a function δ and fit with a parabola. The single crystal elastic coefficients were then calculated by taking the 2nd derivative of the parabolic fit at $\delta = 0$ and using

$$\frac{\partial^2 U^{\text{tet}}}{\partial \delta^2} = \frac{3}{2}(C_{11} - C_{12}) = 3C', \tag{4}$$

$$\frac{\partial^2 U^{\text{tri}}}{\partial \delta^2} = 4C_{44}. \tag{5}$$

Five different tetragonal and five trigonal distortions were used to calculate the corresponding single crystal elastic coefficients.

2.2 Analytic homogenization – Voigt, Reuss, and self-consistent The procedure to estimate polycrystalline elastic properties begins by first estimating the polycrystalline bulk modulus (B^*) and shear modulus (G^*) from single crystal values. Assuming that all possible grain orientations are equally likely (i.e. a non-textured material), both B^* and G^* can be used to calculate Young's modulus (Y^*)

and Poisson's ratio (ν^*) for an elastically isotropic polycrystal via well-established elasticity relations.

The upper bound on B^* and G^* was first calculated by Voigt [9] based on the assumption that during elastic deformation a polycrystal adopts a local uniform strain state. The lower bound on B^* and G^* was calculated by Reuss [10] based on the assumption that during elastic deformation the polycrystal adopts a local uniform stress state. The uniform strain and stress assumptions used by Voigt and Reuss represent two extremes that are rarely observed.

For materials with cubic symmetry, the Voigt and Reuss bounds on B^* (B_V^* and B_R^* respectively) are identical meaning that the polycrystalline bulk modulus is equal to the single crystalline bulk modulus

$$B_V^* = B_R^* = B_{cubic} = B^* . \tag{6}$$

The Voigt and Reuss bounds on the polycrystalline shear modulus (G_V^* and G_R^* respectively) for materials with cubic symmetry depend on the single crystal elastic coefficients via

$$G_V^* = \frac{C_{11} - C_{12} + 3C_{44}}{5}, \tag{7}$$

$$G_R^* = \frac{5}{4(S_{11} - S_{12}) + 3S_{44}}, \tag{8}$$

where C_{ij} are terms in the stiffness matrix and $S_{ij} = C_{ij}^{-1}$.

A more realistic estimate of G^* can be made by employing a self-consistent scheme. Hershey [11] derived a closed form solution to the self-consistent homogenization of the shear modulus (G_{SC}^*) for materials with cubic symmetry. He made the following assumptions about the polycrystal: (i) it was composed of spherically shaped grains; (ii) each grain in the polycrystal was the same size (a uniform grain size distribution); (iii) the grain orientation distribution was random (a non-textured polycrystal). From these assumptions, Hershey showed that G_{SC}^* could be calculated by solving the following quartic equation

$$\begin{aligned} &64G_{SC}^{*4} + 16(4C_{11} + 5C_{12})\, G_{SC}^{*3} \\ &+ [3(C_{11} + 2C_{12})\,(5C_{11} + 4C_{12}) - 8(7C_{11} - 4C_{12})\, C_{44}]\, G_{SC}^{*2} \\ &- (29C_{11} - 20C_{12})\,(C_{11} + 2C_{12})\, C_{44} G_{SC}^{*} \\ &- 3(C_{11} + 2C_{12})^2\,(C_{11} - C_{12})\, C_{44} = 0 . \end{aligned} \tag{9}$$

Once homogenized values of G^* and B^* have been estimated, other elastic properties of an elastically isotropic polycrystalline aggregate can also be calculated with standard elasticity relations. In particular, Y^* and ν^* are

$$Y^* = \frac{9B^*G_x^*}{3B^* + G_x^*}, \qquad \nu^* = \frac{1}{2}\frac{3B^* - 2G_x^*}{3B^* + 2G_x^*}, \tag{10}$$

where G_x^* can be G_R^*, G_V^*, or G_{SC}^*.

2.3 Finite element method homogenization

Polycrystalline elastic properties were calculated using the the anisotropic elastic material routine within the commercial finite element code MSC.Marc200×. In order to investigate the effect of grain size distribution, two different polycrystals were meshed and simulated. The first polycrystal contained 96 ($4 \times 6 \times 4$) equally shaped square grains. Each grain was meshed with 27 quadratic brick elements resulting in a mesh with 2592 total elements. The second polycrystal contained 84 grains of varying sizes and shapes. This microstructure was generated by performing a Potts Monte Carlo simulation of normal, ideal grain growth starting from a random distribution of voxels. The grain size distribution in this "realistic" microstructure was log-normal where the average number of elements per grain was around 49 and the median number of elements per grain was 37. All the grains in this polycrystal were meshed with quadratic brick elements and the resulting mesh had a total of 4096 elements. Both the square grain and non-uniform grain size polycrystal meshes are shown in Fig. 2. In both polycrystals, each grain was assigned a random orientation and the elasticity tensor (C_{ij}) containing the single crystal elastic coefficients was then rotated into the corresponding grain's orientation (i.e. the $C_{ij}s$ in each grain differed only by a rotation).

The FEM determined polycrystalline Young's modulus (Y_{FEM}^*) and Poisson's ratio (ν_{FEM}^*) were calculated by simulating a uniaxial tensile test. A fixed displacement normal to the y-direction in the polycrystal was prescribed while displacements on three other orthogonal planes were fixed to prevent the mesh from translating. The overall stress–strain response was then calculated from the nodal reaction forces and displacements. Furthermore, because polycrystals containing around 100 grains constitutes a small statistical population, the stress-strain response at each alloy concentration was simulated 5 times using the same polycrystalline mesh but with a different random orientation distribution. An average Y_{FEM}^* and ν_{FEM}^* was then calculated from these 5 simulations to approximate a random orienta-

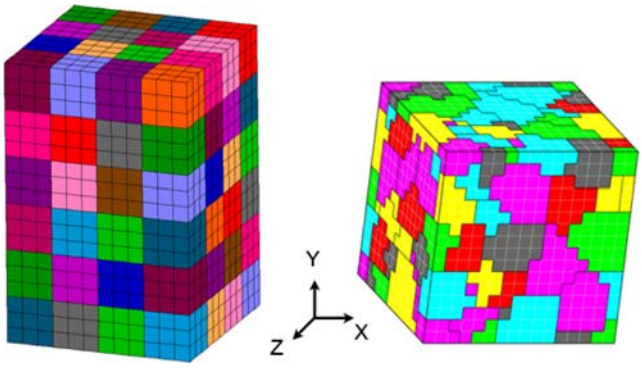

Figure 2 (online colour at: www.pss-b.com) 96 square shaped grain polycrystal mesh and the 84 non-uniform grain shape polycrystal mesh used in the FEM simulations.

tion distribution. Finally, G^*_{FEM} could be calculated assuming elastic isotropy

$$G^*_{FEM} = \frac{E^*_{FEM}}{2(1+\nu^*_{FEM})}. \quad (11)$$

3 Results Single crystal elastic coefficients for ordered BCC Mg–Li alloys with compositions ranging from 0–100 at% Li were calculated using ab initio methods. It should be noted that BCC Mg–Li alloys are thermodynamically stable for Li concentrations greater than 30 at% [12]. Nevertheless, the BCC elastic properties for both single and polycrystals were predicted in regions where the BCC crystal structure is not stable in order to derive the complete trends on their concentration dependence. The variation of C_{11}, C_{12}, and C_{44} for single crystals is shown in Fig. 3. While there is little literature data available to validate these single crystal elastic coefficients, it is possible to compare ab initio calculated and experimental single crystal elastic coefficients for pure BCC Li at 78 K [13]. The difference between the experimental and predicted elastic components is small, between 1–6% (or approximately 1 GPa).

These single crystal elastic coefficients were then used as the basis for all the analytic and FEM estimates of polycrystalline elastic properties. The dependence of Y^*, G^*, and ν^* as a function of Li content are shown in Figs. 4 and 5. In each case, the Voigt and Reuss bounds form upper and lower bounds, as should be the case. The difference between these two bounds varies between 20–130% for G^* and Y^* and 25–50% for ν^*. Such large differences between the upper and lower bounds illustrate that these bounds by themselves do not necessarily restrict the polycrystalline elastic properties to a small-sub set from which reasonable values can be extracted. Interestingly enough, the self-consistent and FEM predictions fall close to the midpoint between upper and lower bounds. This result validates Hill's [14] suggestion that B^* and G^* can be reasonably estimated by taking an arithmetic mean of the upper and lower bound.

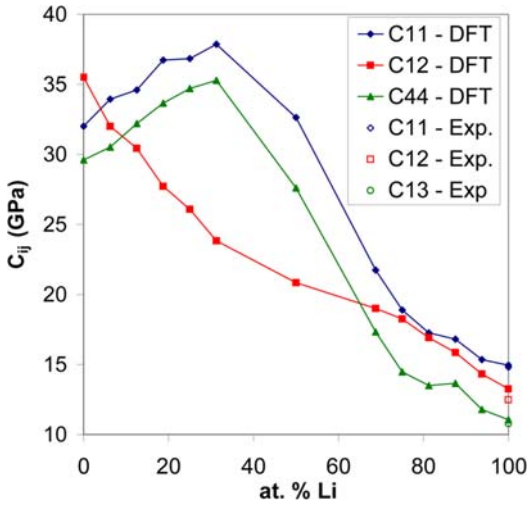

Figure 3 (online colour at: www.pss-b.com) Dependence of the ab initio calculated single crystal elastic coefficients for BCC Mg–Li alloys on lithium concentration. Experimental Li data at 78 K is from Nash and Smith [13].

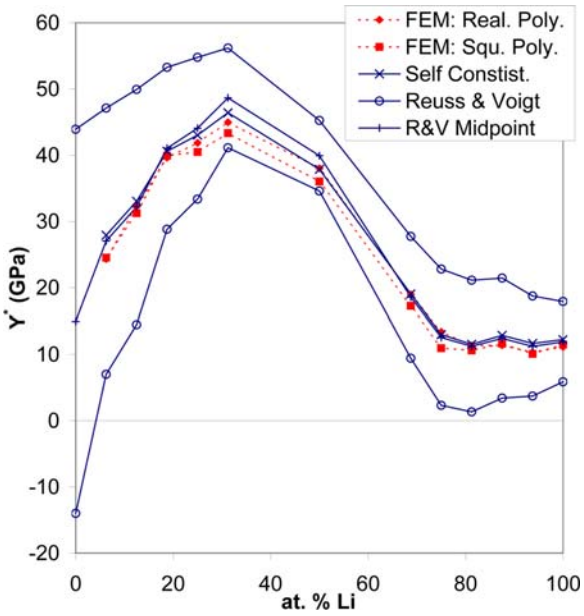

Figure 4 (online colour at: www.pss-b.com) Compositional dependence of Young's modulus for polycrystalline BCC Mg–Li alloys with a random texture. Red dashed lines indicate FEM calculations, and blue solid lines analytic ones.

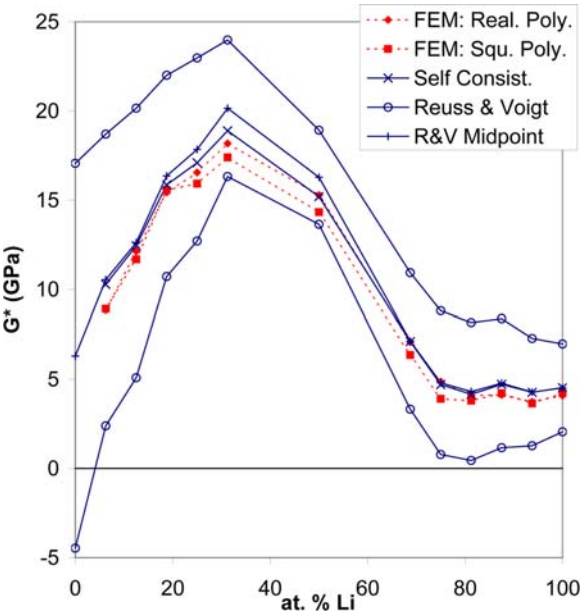

Figure 5 (online colour at: www.pss-b.com) Compositional dependence of shear modulus for polycrystalline BCC Mg–Li alloys with a random texture. Red dashed lines indicate FEM calculations, and blue solid lines analytic ones.

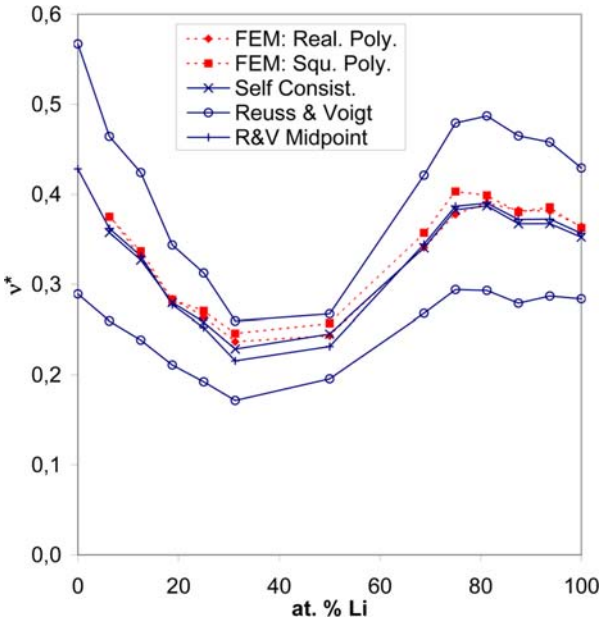

Figure 6 (online colour at: www.pss-b.com) Compositional dependence of Poisson's ratio for polycrystalline BCC Mg–Li alloys with a random texture. Red dashed lines indicate FEM calculations, and blue solid lines analytic ones.

In Figs. 4 and 5, the Voigt and Reuss approaches estimate polycrystalline elastic properties for BCC Mg, but the self-consistent and FEM approaches do not. In the self-consistent case, all of the roots to Eq. (9) are imaginary; while for FEM, the simulations crash immediately due to a non-positive definite stiffness matrix. The self-consistent and FEM methods are unable to calculate real elastic modulus values in cases when C' (defined in Eq. (4)) is negative, as is the case for BCC Mg. When C' is negative, it indicates that both the single crystal and polycrystalline form of the material is mechanically unstable. In other words, BCC Mg will undergo a phase transformation upon the application of strain. The negative G_V^* and Y_V^* also hints at this mechanical instability. These results are in agreement with the ab initio Bain path calculations by Jona and Marcus [15].

The polycrystalline elastic properties predicted by the self-consistent approach do not differ greatly from those predicted by FEM. FEM in general predicts a slightly lower modulus value and a slightly higher ν^* value. The difference between the predicted G^* and Y^* values from both approaches was between 2–17% and between 0–4% for ν^*. Because the Mg–Li alloy system has low polycrystalline elastic modulus values in the Li rich region, the *relative* differences between the self-consistent and FEM values can be large. However, the *absolute* differences between the two approaches is reasonable: 1–3 GPa for shear and Young's modulus and between 0.003–0.02 for Poisson's ratio. The ability to predict similar polycrystalline elastic properties using a quartic equation (solved instantly) and FEM (solved on the order of minutes to hours) illustrates the power and value of the self-consistent approach.

Table 1 Comparison of polycrystalline elastic properties predicted by the self-consistent and FEM approaches.

	FEM square grains vs. self-consistent	FEM non-uniform grains vs. self-consistent
ΔG range (GPa)	0.30–1.50	0.03–0.71
ΔG avg. (GPa)	0.72	0.35
ΔY range (GPa)	0.68–3.07	0.07–1.48
ΔY avg. (GPa)	1.66	0.82
$\Delta\nu$ range	0.003–0.020	0.000–0.015
$\Delta\nu$ avg.	0.013	0.007

A comparison of the polycrystalline elastic properties predicted by FEM using a uniform and non-uniform grain size distribution reveals that using a non-uniform grain (i.e. more realistic) size distribution results in elastic properties that are closer to the self-consistent predictions. The differences between G^*, Y^*, and ν^* for both FEM approaches and the self-consistent approach are summarized in Table 1. In general, the FEM predictions using a non-uniform grain size polycrystal are 50% closer to the self-consistent results than the FEM results based on a polycrystal containing a uniform grain size. At first glance, this trend may be regarded as unexpected since the self-consistent approach was derived from a polycrystal with a uniform spherical grain size distribution. However, FEM simulations based on a more realistic polycrystal mesh should lead to a better prediction of polycrystalline elastic properties. Therefore, the fact that the better FEM predictions lie closer to the self-consistent results further validates the self-consistent approach.

4 Conclusions Single crystal elastic coefficients (C_{11}, C_{12}, and C_{44}) were predicted for 11 BCC Mg–Li alloys as well as BCC Mg and Li using ab initio methods. A multiscale approach that bridged the atomistic and macroscale levels was employed to estimate polycrystalline elastic properties (Y^*, G^*, and ν^*) using both analytic homogenization and FEM methods. As expected, the upper and lower bounds for each of the polycrystalline elastic properties was defined by the Voigt and Reuss solutions. While the difference between these two bounds was too large to be useful, the arithmetic mean of the two bounds did provide a reasonable approximation.

For elastically isotropic materials with cubic symmetry and a random grain orientation distribution (i.e. non-textured materials), the difference between the polycrystalline elastic properties predicted using and FEM and those predicted using an analytic self-consistent approach is small. Y^* and G^* computed using FEM were 1–3 GPa smaller than those computed using the analytic self-consistent approach, while the FEM based values for ν^* were 0.00–0.15 higher. The effect of grain size distribution on the FEM results was also investigated. The FEM

predictions using a non-uniform grain size polycrystal are 50% closer to the self-consistent results than the FEM results based on a polycrystal containing a uniform grain size. The good agreement between the polycrystalline elastic properties derived from the self-consistent approach and FEM illustrates the power and value of applying the self-consistent approach to materials with cubic symmetry.

Acknowledgement We thank the "Triple M Max Planck Initiative on Multiscale Modeling of Condensed Matter" for financial support.

References

[1] D. Raabe, B. Sander, M. Friák, D. Ma, and J. Neugebauer, Acta Mater. **55**, 4475–4487 (2007).
[2] P. Hohenberg and W. Kohn, Phys. Rev. **136**, B864 (1964).
[3] W. Kohn and L. J. Sham, Phys. Rev. **140**, A1133 (1965).
[4] G. Kresse and J. Hafner, Phys. Rev. B **47**(1), 558–561 (1993).
[5] G. Kresse and J. Furthmüller, Phys. Rev. B **54**(16), 11169–11186 (1996).
[6] J. P. Perdew, K. Burke, and M. Ernzerhof, Phys. Rev. Lett. **77**, 3865 (1996).
[7] P. E. Blöchl, Phys. Rev. B **50**(24), 17953–17979 (1994).
[8] K. Chen, L. R. Zhao, and J. S. Tse, J. Appl. Phys. **93**(3), 2414–2417 (2003).
[9] W. Voigt, Lehrbuch der Kristallphysik (Teubner, Stuttgart, 1928).
[10] A. Reuss, Z. Angew. Math. Mech. **9**, 49 (1929).
[11] A. V. Hershey, J. Appl. Mech. **9**, 49 (1954).
[12] T. Massalski, Binary Alloy Phase Diagrams (ASM International, 1990).
[13] H. Nash and C. Smith, J. Phys. Chem. Solids **9**, 113 (1959).
[14] R. Hill, Proc. Phys. Soc. Lond. A **65**, 349 (1952).
[15] F. Jona and P. M. Marcus, Phys. Rev. B **66**, 094104 (2002).